Loss of PINK1 promotes the expansion of hematopoietic cells via upregulating autophagy

Zhen-Ni Yi
The Hong Kong Polytechnic University
Xiang-Ke Chen
The Hong Kong Polytechnic University
Alvin Chun-Hang Ma (alvin.ma@polyu.edu.hk)
The Hong Kong Polytechnic University

Article

Keywords:

Posted Date: April 10th, 2023

DOI: https://doi.org/10.21203/rs.3.rs-2671385/v1

Additional Declarations: No competing interests reported.

Loss of *PINK1* promotes the expansion of hematopoietic cells via upregulating autophagy

Short title: Loss of PINK1 promotes hematopoiesis.

Zhen-Ni Yi[1,#], Xiang-Ke Chen[1,#], and Alvin Chun-Hang Ma[1]

[1]Department of Health Technology and Informatics, Faculty of Health and Social Sciences, The Hong Kong Polytechnic University, Hung Hom, Hong Kong, China

[#]These authors contributed equally to this work

Address for correspondence:

Dr. Alvin Chun-Hang MA, Ph.D.

Rm. Y928, Lee Shau Kee Building, The Hong Kong Polytechnic University,

Hung Hom, Hong Kong, China.

Tel: +852 34008913.

Fax: +852 23624365.

E-mail: alvin.ma@polyu.edu.hk

Word count (main text): 1982

Word count (abstract): 158

Figure/table count: 5

Reference count: 48

Abstract

PTEN-induced putative kinase 1 (PINK1) is a well-characterized regulator of mitochondrial quality control through mitophagy and its mutations are associated with recessive Parkinson's disease. However, little is known about its functions in normal and malignant hematopoiesis in vertebrates. Here we aim to unravel the roles of PINK1 in definitive hematopoiesis and its underlying mechanisms using zebrafish (*Danio rerio*). In this study, we utilized CRISPR/Cas9 system to generate *pink1* knockout zebrafish model and *PINK1*-deficient leukemia cell line. We found that *pink1* deficiency activated autophagy in hematopoietic cells and promoted definitive hematopoiesis in zebrafish embryos, which can be alleviated by canonical autophagy inhibition. Further, the proteomic and metabolic analysis revealed an elevated expression of cell proliferation markers and enhanced respiration in *pink1*-deficient zebrafish embryos. On the other hand, *PINK1* deficiency also induced autophagy and cell proliferation in human leukemic cells. Therefore, our findings demonstrated that PINK1 functions as a negative regulator of normal and malignant hematopoiesis through the autophagy-mediated pathway.

Introduction

PTEN-induced putative kinase 1 (PINK1) is a mitochondrial-targeted serine/threonine kinase, which mediates mitochondrial quality control and promotes cell survival under stress conditions [1,2]. It senses mitochondrial quality and activates the lysosome-dependent degradation pathway for the selective turnover of damaged and superfluous mitochondria[3], namely mitophagy, a selective form of macroautophagy (referred to hereafter as autophagy). In addition, PINK1 also exerts a critical role in canonical autophagy, where its deficiency increases canonical autophagy *in vitro* through interacting with Beclin 1 (BECN1)[4,5]. Loss-of-function mutations in *PINK1* induce Parkinson's phenotypes in animal models[6] and studies suggested that PINK1 implicates the pathogenesis of Parkinson's disease through signaling mitochondrial dysfunction to Parkin-mediated selective autophagy[7]. However, *PINK1*-deficient animal models[8] showed no or minimal alterations in basal mitophagy, significant differences in mitophagy were only observed in the pancreatic cells of *Pink1*-deficient mice[9]. These findings suggested that *PINK1* is either dispensable to basal mitophagy or mediates basal mitophagy and autophagy in a tissue-dependent manner.

Autophagy and mitophagy have long been suggested to involve in normal and malignant hematopoiesis. Ablation of core canonical autophagy-related genes (ATGs), such as *ATG7*, *ATG5*, and *FAK family kinase-interacting protein of 200 kDa* (*FIP200*), resulted in the loss of hematopoietic stem cells (HSCs) and impaired hematopoiesis[10–12]. In particular, mitophagy has been shown to regulate mitochondrial clearance in HSCs to maintain their quiescence and self-renewal[13]. On the contrary, *ATG12* deficiency showed no effect on the hematopoiesis in mice, while it altered the metabolic state of HSCs[14]. In addition to normal hematopoiesis, abnormal autophagy and mitophagy were also observed in leukemic cell lines[15,16] and dual roles of autophagy in oncogenesis and drug resistance were widely reported[17–19]. While the differential phenotypes observed in normal and malignant hematopoiesis can be attributed to specific functions of different ATGs-mediated non-canonical autophagy[20], a comprehensive picture of various ATGs regulating both normal and malignant hematopoiesis is needed. As one of the known regulators of mitophagy, the roles of *PINK1* in normal and malignant hematopoiesis remains largely unknown. Therefore, here we aim to investigate the functions and

underlying autophagy-mediated mechanisms of *pink1* in regulating normal and malignant hematopoiesis using zebrafish (*Danio rerio*) model and leukemic cell lines.

Results

Targeting *pink1* induces autophagy in the muscle and hematopoietic cells of zebrafish embryos

Zebrafish *pink1* composes of 8 exons, encoding 574 amino acids, and the encoded protein share around 70% homology with the human *PINK1* in the kinase domain (Fig. 1a). To study the function of *PINK1* in hematopoiesis, we generated *pink1* knockout zebrafish mutant (*pink1*^{Mut}) embryos by targeting *exon-3* of zebrafish *pink1* using the CRISPR/cas9 gene editing method (Fig. 1b). Over 90% mutagenic efficiency was confirmed by restriction fragment length polymorphism (RFLP) assay in RNP-injected embryos (Fig. 1c and Suppl. Fig. S2a), similar to previous reports that bi-allelic mutation could be achieved in F0 embryos through CRISPR/cas9[21,22]. Sanger sequencing demonstrated that majority of *pink1*^{Mut} carried a 4 bp deletion, which is expected to cause frameshift truncation (Suppl. Fig. S1a). Significant decrease in pink1 protein level was also confirmed by western blot (Fig. 1d, e and Suppl. Fig. S2b). While *pink1*^{Mut} showed normal morphology and viability during early embryonic stages, the level of Lc3-II significantly increased comparing with control at 48 hour-past-fertilization (hpf) (Fig. 1e). We further examined the autophagic changes in various tissues using Tg(*Lc3*:GFP) reporter line with LysoTracker Red co-staining. The number of GFP-Lc3 vacuoles in muscle increased in *pink1*^{Mut} embryos comparing with controls (Fig. 1f). With LysoTracker Red co-staining, the average number of autolysosomes and lysosomes also increased in the muscle of *pink1*^{Mut} ($p<0.01$, n=20-40 areas quantified, Fig. 1g). To examine autophagic changes in hematopoietic cells of zebrafish embryos, Tg(*coro1a*:DsRed) reporter line with Cyto-ID staining was used (Fig. 1h) and increased number of Cyto-ID+ autophagic vacuoles was also observed in DsRed+ hematopoietic cells of *pink1*^{Mut} embryos (Fig. 1i, j).

Knockout of *pink1* promotes definitive hematopoiesis in zebrafish embryos

Whole mount in situ hybridization (WISH) of various hematopoietic markers were performed to analyze definitive hematopoiesis in *pink1*^{Mut} embryos. As shown by the WISH results, the hematopoietic stem cell

(HSC) population (*c-myb*), pan-leukocyte population (*l-plastin*) and erythroid population (*hbae1*) significantly increased in *pink1*^{Mut} compared with controls (Fig. 2a, b, d), while no significant change was observed in neutrophil population (*mpx*) (Fig. 2c). To investigate the potential link between the observed phenotypes in autophagy and hematopoiesis, we conducted rescue experiments by treating zebrafish embryos with 3-MA, an early-stage autophagy inhibitor. While 3-MA treatment on its own only produce subtle changes in various hematopoietic populations, it significantly ameliorated the expansion of HSC, pan-leukocyte, and erythroid populations in *pink1*^{Mut} embryos (Fig. 2a-e). Though neutrophil population was not significantly affected by 3-MA treatment or *pink1* mutation, concomitant *pink1* mutation and 3MA-treatment significantly perturbed the neutrophil population (Fig. 2c, e). These results suggested that pink1 may function as a negative regulator in hematopoiesis via suppressing autophagy in hematopoietic cells.

Knockout of *pink1* increases oxidative phosphorylation and altered mitochondria morphology in zebrafish embryos

To investigate the bioenergetics associated with *pink1* loss-of-function mutation in zebrafish embryos, we performed mitochondrial stress test in live embryos with Seahorse XF24 Analyzer. Cellular oxidative phosphorylation (OXPHOS) and glycolysis were measured by recording the oxygen consumption rate (OCR), an indicator of respiration, in real-time during consecutive injections of 25 µM oligomycin, 2.5 µM FCCP, and 1 µM rotenone/antimycin A (Fig. 3a, b). The data showed that *pink1*^{Mut} exhibited elevated basal and maximal respiration aa well spare respiratory capacity comparing with WT controls (Fig. 3c, d, g). The ATP production did not change while the coupling efficiency significantly decreased in *pink1*^{Mut} embryos (Fig. 3e, f), suggesting that efficiency of mitochondria was affected. By injecting mitoRed mRNA into *mfaap4*:BFP zebrafish embryos, we also observed the enlargement of mitochondria in macrophage of *pink1*^{Mut}, with the loss of boundary and increased connectivity of individual mitochondrion (Fig. 3h, i). Overall, *pink1*^{Mut} embryos demonstrated a promotion in mitochondrial activity while decreased efficiency compared to the WT siblings. Loss-of-function *pink1* mutation promoted cell proliferation and cell metabolism, while impairing complexes efficiency for ATP production.

Knockout of *pink1* promotes cell proliferation and DNA metabolism in zebrafish embryos

Mass spectrometry-based proteomics was used to examine proteomic changes in zebrafish embryos upon *pink1* knockout (Fig. 4a). A total of 106 proteins with significantly change (80 upregulated, 26 downregulated, $p < 0.05$ and fold change > 1.2) were identified in $pink1^{Mut}$ (Fig. 4b). Pathway analysis revealed that cell cycle, proliferation, mitochondrial, and metabolism pathways were significantly altered in $pink1^{Mut}$ (Fig. 4c-e). To verify the proteomic profiling, western blot was performed to confirm the decrease of cytochrome c (key component of the electron transport chain in mitochondria) and TP16 variants (tumor suppressor) in $pink1^{Mut}$, while RAC1 (activator of cell growth and migration), and beclin1 (key component of autophagy) were significantly increased in $pink1^{Mut}$ embryos (Suppl. Fig. S1b, c and S3).

Targeting *PINK1* induces cell proliferation and autophagy in acute myeloid leukemia (AML) cells

To further investigate the potential roles of *PINK1* in malignant and human hematopoiesis, we generated *PINK1*-deficient OCI-AML3 leukemic cell line by CRISPR/Cas9 (Fig. 5a). RFLP assay and Sanger sequencing confirmed the mutant leukemic cells carried a 1 bp frame-shifting insertion mutation in *PINK1* (Fig. 5b, Suppl. Fig. S1a and Suppl. Fig. S2c). A significant decrease in PINK1 protein expression was confirmed by western blot (Fig. 5c, d and Suppl. Fig. S2d). Autophagic flux in *PINK1*-deficient leukemic cells were examined by flow cytometry and imaging with Cyto-ID staining. The number of autophagic vacuoles per cell was markedly elevated in *PINK1*-deficient leukemic cells (Fig. 5e-h). However, according to RT-qPCR, no significant change was found among other autophagic genes such as ATG3, ATG5, or ATG7 (Suppl. Fig. S1d). Consistent with the observation in zebrafish model, *PINK1*-deficient cells also exhibited a higher proliferation rate comparing with controls, as well as lower expression of TP53 (Fig. 5i, Suppl. Fig. S1d). Notably, CQ-treatment significantly rescued the enhanced proliferation in *PINK1*-deficient leukemic cells without affecting the basal proliferation in controls. These results suggest that *PINK1* potentially regulates proliferation in leukemic cell through modulating autophagy.

Discussion

Autophagy plays an important role in cell proliferation and survival under adverse conditions. Shortage of nutrients induced autophagy during neonates development while knockout of the autophagy genes results in animal death[23]. The elevated expressions of key autophagic genes, for example *ATG7* and *BECN1*, are associated with poor recovery and short remission of AML patients [24]. Deficiency in autophagic genes like *ATG5* or *ATG7* impair normal development of hematopoietic stem cells[11] and leads to myeloid expansion[25]. Here we make use of the zebrafish model to investigate the previously undescribed role of *Pink1* in normal and malignant hematopoiesis. We introduced frameshifting mutation in zebrafish *pink1* by high efficiency CRISPR/Cas9 RNP. Although F0 *pink1*^{Mut} cannot survive into reproductive adulthood, bi-allelic mutation could be achieved in embryos injected with RNP to allow phenotypic analysis in F0 embryos. While *pink1* knockout induced abnormal expansion of hematopoietic stem cells, erythroid cells, and pan-leukocytes in zebrafish embryos, autophagy in various embryonic tissues, including hematopoietic cells were also elevated in *pink1*-deficient zebrafish embryos. More importantly, treatment with 3-MA, a potent autophagy inhibitor, could rescue the hematopoiesis phenotypes in *pink1*^{Mut}, indicating *pink1* regulates normal hematopoiesis via autophagy. *PINK1* deficiency also enhanced autophagy and cell proliferation in AML cell line, which can be alleviated by autophagy inhibition with CQ. This suggested that the elevated cell proliferation in *PINK1*-deficient leukemic cells is likely due to up-regulation of canonical autophagy. Collectively, our findings demonstrated that *PINK1* plays a conserved role in both normal and malignant hematopoiesis in vertebrate through regulating canonical autophagy.

Previous studies have reported the role of mitochondria and mitophagy in the homeostasis of hematopoietic progenitor cells, in particular, the role of Parkin-dependent mitophagy in the expansion of hematopoietic stem cells[26]. Bone marrow cells from *Pink1* knockout mutant mice showed increased mitochondrial respiration and faster development[27]. Mitochondria adapt to the metabolic rates of cells by fission, fusion, and mitophagy. Mitochondria undergo biogenesis and fusion when the metabolic demand increases, while opposite mitochondrial fission and mitophagy occurs when the metabolic demand decreases[28]. It is reported that loss

of PINK1 results in increased reactive oxygen species (ROS) levels, enhanced lipid peroxidation and glutathione metabolism, defected complex I activity, reduced uptake of calcium, impaired ATP production, an elevated cytochrome C release *in vitro*[29–31]. Impaired mitochondrial function and altered morphology (swollen and enlarged mitochondria) have also been described in animal models and patient tissues[32–35]. Consistent with previous studies, we observed abnormal mitochondria in *pink1* deficient zebrafish embryos. Proteins related to oxidative phosphorylation and electron transport chain, including mitochondrial complex I, cytochrome c, and ATP synthase subunits were significantly downregulated in *pink1*^{Mut}, supporting the conserved function of PINK1 in maintaining mitochondrial structures and functions (Fig. 4c). In addition, oxidative respiratory was upregulated in *pink1*^{Mut}. Even with elevated basal respiration, maximal respiration, the mitochondrial efficiency was found largely reduced in *pink1*^{Mut}. These results suggest that loss of pink1 might promoted cell proliferation, metabolism, and overall mitochondrial activity, even though with a deficient mitochondria function. The metabolomics alterations in the *pink1*^{Mut} might be due to the increased autophagy and cell proliferation.

Mitophagy is a regulatory mechanism of AML progression. Some studies suggested disrupted mitophagy causes loss of leukemic stem cells, while impaired mitophagy is correlated with poor murine myeloid leukemia progression[18,36]. Treatments with the conventional autophagy inhibitors such as CQ, bafilomycin A1, and Lys05 can attenuate mitophagy/autophagy and inhibit leukemia cell growth with significantly increased expression of *PINK1*[37], which suggests PINK1 as a potential therapeutic target in AML treatment. Here we reported the conserved mitochondrial-regulatory function of pink1 in zebrafish model and evidenced the expanded hematopoiesis as well as upregulated autophagy in *pink1*^{Mut}. However, the underlying cellular mechanism of how pink1 regulates autophagy and how upregulated autophagy promotes hematopoiesis remain largely unknown. Interactions between Pink1 and other candidate proteins, such as TP16, TP53, BECN, and RAC1 warrants further investigation. Nevertheless, with the advancement of zebrafish modelling in hematopoiesis and leukemia[38,39], our study demonstrated the potential of zebrafish model to further investigate the novel role of Pink1 in vertebrate autophagy and hematopoiesis *in vivo*.

Methods

Zebrafish husbandry and maintenance

Wild-type, Tg(*Lc3*:GFP), Tg(*mfap4*), Tg(*coro1a*:DsRed), and mutant zebrafish lines were maintained under standard aquatic conditions and fed twice a day with living shrimp. Embryos were collected from natural spawning and were staged by the hour past fertilization (hpf) according to the morphology criteria described previously[40]. All animal experiments were approved by the Animal Subjects Ethics Sub-Committee (ASESC) of The Hong Kong Polytechnic University and all methods were performed in accordance with the relevant guidelines and regulations. In addition, all studies involving live animal reported in accordance with the Animal Research: Reporting In Vivo Experiments (ARRIVE) guidelines.

Gene editing via CRISPR/Cas9 system

Cas9 nuclease and synthesized sgRNA were purchased from the Integrated DNA Technologies (Iowa, USA). The products were stored at -20 °C upon receival. Cas9 nuclease and diluted sgRNAs were mixed and activated by incubation at 37 °C for 10 minutes to form the ribonucleoprotein (RNP) before microinjection into the one-cell-stage embryos as previously described[41]. For each experiment, the same batch of embryos (around 200 embryos) was divided into the control group and the experimental group for further experiments. Restriction fragment length polymorphism (RFLP) assay and Sanger sequencing were used to check and confirm the mutation. Primer and sgRNA sequences are shown in Supplementary Table S1.

Cell culture and transfection

OCI-AML3 cells were obtained from DSMZ company (Leibniz Institute, Germany). Cells were cultured in RPMI-1640 medium supplemented with 10% fetal bovine serum and 1% penicillin-streptomycin (Thermo Fisher, #72400120, A3160802, and #10378016). The incubator was maintained at 37 °C, with 5% CO2, and sterilized. Cell numbers were counted on an automated cell counter (Invitrogen, USA). Electroporation was performed on the Neon Transfection system with the 100ul kit, with cells concentrated to $5X10^7$/ml, and parameters set

at 1700 v, 20 ms, and 1 pulse (Thermo Fisher, USA). Control and targeted RNP transfected cells were cultured for 2 days. Then cell number was measured for cell viability and proliferation. The mutation was verified between groups by RFLP assay and Sanger sequencing.

Restriction fragment length polymorphism analysis

Embryos at 24 hpf were collected, lysed with gDNA extraction buffer and proteinase K (2 mg/ml, Thermo Fisher, #25530049), followed by 10 minutes, 98 °C inactivation. DNA was amplified using pre-designed primers (Suppl. Table S1). AciI and StyI were ordered from the New England Biolabs (NEB) and stored at -20 °C (NEB, USA). Polymerase chain reaction (PCR)-amplified DNA was subjected to restriction enzyme digestion and run on the 1.5% agarose gel electrophoresis to detect mutations. The batch of mutation-confirmed embryos were used in the following experiments.

Western blot

Embryos (n=30 for each group) were deyolked before being homogenized in protein extraction Reagent (Thermo Fisher, #78501) using an insulin syringe with a needle (BD Biosciences, #324921). Protein concentrations were measured by bicinchoninic acid (BCA) assay kits (Thermo Fisher, #23225) and protein lysates were mixed with 5X sodium dodecyl sulfate (SDS) loading buffer and heat denatured. Protein samples were then electrophoresed on 12% TGX™ FastCast™ Acrylamide Kit (Bio-Rad, #1610175), transferred to polyvinylidene difluoride (PVDF) membrane (Bio-Rad, #1620264) and blocked in 5% non-fat dry milk (Bio-Rad Laboratories, #1706404). Membranes were then hybridized with Lc3b (Abcam, #ab48394; 1:1000), GAPDH (Cell Signaling Technology, #2118; 1:2000), PINK1 (Cell Signaling Technology, #6946, 1:1000), at 4°C overnight. PVDF membranes were further washed in TBST and incubated with goat anti-rabbit or anti-mouse secondary antibody (Abcam, #ab6721, ab6789; 1:3000) for 2 hours at room temperature before signal development with Western ECL Substrate (Bio-Rad, #1705061) and imaging under ChemiDoc XRS+ System (Bio-Rad, USA). ImageJ (NIH) was utilized to measure the relative mass of proteins. Then the Mean gray value was used in statistical analysis.

Whole mount in situ hybridization (WISH)

Anti-sense mRNA probes of *hemoglobin* (*hbae1*), *lymphocyte cytosolic protein 1* (*l-plastin*), *v-myb avian myeloblastosis viral oncogene homolog* (*c-myb*), and *myeloid-specific peroxidase* (*mpx*) were generated by PCR amplification of wild-type zebrafish cDNA, cloning with pGEM®-T Easy vector (Promega Corporation, A1360), in vitro transcription, and labeling with DIG RNA Labeling Kit (Roche, #11175025910). Embryos were fixed with 4% paraformaldehyde (PFA) at room temperature for 4 hours, then dehydrated using ethanol and stored at -20 °C overnight. WISH was performed on fixed zebrafish embryos following protocols as described previously[42]. The first investigator performed the microinjection and was aware of the group allocation. A second investigator performed the WISH but was unaware of the group allocation and responsible for data analysis.

Autophagy modulator treatment, LysoTracker staining and Lightsheet imaging

Embryos at 2 dpf were treated with 100 µM chloroquine (Selleckchem, #S4157) and 10 mM 3-Methyladenine (3-MA) (Selleckchem, #S2767) for 24 hours. Fluorescent dye LysoTracker™ Red DND-99 (Invitrogen, #L7528) targeting lysosomes was diluted to a final concentration of 10µM. Tg(*Lc3*:GFP) zebrafish embryos at 3 dpf were incubated with the solution in dark at 28.5 °C for 45 minutes[43]. Subsequently, embryos were rinsed 3 times with E3 fish water prior to imaging. Lightsheet imaging was done by Zeiss Lightsheet Z.1 Selective Plane Illumination Microscope (Carl Zeiss Microscopy, NY, USA). Images were further processed and analyzed with ZEN (Carl Zeiss Microscopy, NY, USA) software. GFP-Lc3 positive, LysoTracker Red positive, and GFP-Lc3 and LysoTracker Red double-positive puncta were counted from the selected brain and muscle sections to measure the relative autophagosome, lysosome and autolysosome numbers (20 out of 100 layers), following the criteria described in the previous study[44].

Flow cytometry and Fluorescence-activated cell sorting (FACS)

Tg(*coro1a*:DsRed) zebrafish embryos at 3 dpf were digested with Trypsin-EDTA (0.05%) (Thermo Fisher, #25300062) for 15 minutes at 28°C and then dissociated with pipetting on ice. After termination of Trypsin

with CaCl2 (2mM), the suspension was filtered using a 40 µm cell strainer (BD Biosciences, #352340) and washed with phosphate-buffered saline (PBS) solution supplemented with 1% fetal bovine serum (FBS) (Thermo Fisher, 26140079). FACS of coro1a + leukocytes were then conducted in BD FACSAria III Cell Sorter according to the manufacturer's instructions.

CYTO-ID staining and Confocal imaging

Sorted *coro1a*+ cells were stained with Cyto-ID and Hoechst (Enzo Life Sciences, USA), and incubated at 28.5 °C for 30 minutes, avoiding light. After 5 minutes of washing with PBS, cells were plated on the 35 mm glass bottom confocal dish (SPL life sciences, #100350) and imaged by Leica TCS SPE Confocal Microscope (Leica Microsystems, Wetzlar, Germany) with the 40× objective lenses. Images were analyzed using Leica LAS-X software (Leica Microsystems, Wetzlar, Germany).

Liquid chromatography/Electrospray ionization (LC/ESI) Mass spectrometry

Zebrafish embryos (n=30 embryos for each group) at 48 hpf were dissociated and lysed to extract the proteins (Thermo Fisher, #78501). The protein samples were then purified, reduced, alkylated, and digested with trypsin (protein: trypsin=40:1, Promega, V511). The digested peptides were desalted using C18 columns (Thermo Fisher, P189870). Peptides were put on a Thermo scientific liquid chromatography system connected to a linear Trap-Orbitrap hybrid mass spectrometer (LTQ-Orbitrap XL, Thermo Fisher Scientific, Bremen, Germany) with electrospray ionization (ESI). Detailed parameters were described elsewhere[45,46]. After data analysis, we obtained the values of p-values (in -log 10) and z-scores (in log 2) in around 3000 quantified proteins between the wildtype (WT) control and the mutant (Mut) embryos.

Real time quantitative PCR (RT-qPCR)

Total RNA was extracted from embryos using RNAiso Plus (Takara, #9108). cDNA was synthesized using RevertAid First Strand cDNA Synthesis Kit (Thermo Fisher, K1622) in accordance with the manufacturer's protocol. The cDNA was then mixed with FastStart Universal SYBR Green Master (Roche, #4913850001)

reagents (Suppl. Table S1). PCR with the standard program was performed on ABI 7300 Real-Time PCR System (Thermo Fisher, USA).

Sea horse and mitochondria stress test

Zebrafish embryos at 48 hpf were placed in a 24-well plate, one embryo per well, and pressed to the bottom with a net, kept at 28.5 °C. XF24 Analyzer was used to perform the experiment (Seahorse Bioscience Inc., USA). A final concentration of 25 µM oligomycin (Sigma Aldrich, 1404-19-9), 2.5 µM carbonyl cyanide 4-(trifluoromethoxy) phenylhydrazone (FCCP, Sigma Aldrich, 370-86-86), 1 µM antimycin-A (Sigma Aldrich, 1397-94-0) and 1 µM rotenone (Sigma Aldrich, R8875) were injected consecutively into a final volume of 700 µL E3 medium per well. Oxygen consumption rate (OCR) was recorded at various time points following the standard program as previously described[47,48]. Basal respiration was calculated on the last three-point OCR before the injection of oligomycin. Non-mitochondrial oxygen consumption rate is measured by the minimum reading after rotenone/antimycin A injection. Maximal respiration was the maximum OCR measurement following exposure to the mitochondrial uncoupler FCCP. Proton leak was calculated by OCR after oligomycin injection minus the OCR after rotenone/antimycin A injection. Adenosine triphosphate (ATP) production is measured by the last OCR before oligomycin injection minus the minimum rate after oligomycin injection. Coupling efficiency is calculated by dividing ATP production rate with basal respiration rate. Finally, spare respiratory capacity is calculated by dividing maximal respiration by basal respiration. The experiment was repeated three times in the exact same conditions.

Statistics analysis

Statistical analysis was performed by unpaired, two-tailed Student's t-test using GraphPad Prism, version 8 (GraphPad Software, CA, USA). Error bars represent the standard error of the mean. Data were presented as mean ± standard error of the mean (SEM) and P-value less than 0.05 ($P < 0.05$) were considered statistically significant.

Data sharing statement

The data generated and analyzed during the current study are available from the corresponding author upon reasonable request. Sequencing data are available in the DDBJ repository, [LC760345 (http://getentry.ddbj.nig.ac.jp/getentry/na/LC760345/?filetype=html)] and [LC760346 (http://getentry.ddbj.nig.ac.jp/getentry/na/LC760346/?filetype=html)].

References

1. Valente, E. M. *et al.* Hereditary early-onset Parkinson's disease caused by mutations in PINK1. *Science* **304**, 1158–1160 (2004).
2. Yang, Y. *et al.* Mitochondrial pathology and muscle and dopaminergic neuron degeneration caused by inactivation of Drosophila Pink1 is rescued by Parkin. *Proc. Natl. Acad. Sci. U. S. A.* **103**, 10793–10798 (2006).
3. Youle, R. J. & Narendra, D. P. Mechanisms of mitophagy. *Nat. Rev. Mol. Cell Biol.* **12**, 9–14 (2011).
4. Michiorri, S. *et al.* The Parkinson-associated protein PINK1 interacts with Beclin1 and promotes autophagy. *Cell Death Differ.* **17**, 962–974 (2010).
5. Dagda, R. K. *et al.* Loss of PINK1 function promotes mitophagy through effects on oxidative stress and mitochondrial fission. *J. Biol. Chem.* **284**, 13843–13855 (2009).
6. Park, J. *et al.* Mitochondrial dysfunction in Drosophila PINK1 mutants is complemented by parkin. *Nature* vol. 441 1157–1161 (2006).
7. Narendra, D., Walker, J. E. & Youle, R. Mitochondrial quality control mediated by PINK1 and Parkin: links to parkinsonism. *Cold Spring Harb. Perspect. Biol.* **4**, (2012).
8. Clark, I. E. *et al.* Drosophila pink1 is required for mitochondrial function and interacts genetically with parkin. *Nature* vol. 441 1162–1166 (2006).
9. McWilliams, T. G. *et al.* Basal Mitophagy Occurs Independently of PINK1 in Mouse Tissues of High Metabolic Demand. *Cell Metab.* **27**, 439-449.e5 (2018).
10. Mortensen, M. *et al.* The autophagy protein Atg7 is essential for hematopoietic stem cell

maintenance. *J. Exp. Med.* **208**, 455–467 (2011).

11. Gomez-Puerto, M. C. *et al.* Autophagy Proteins ATG5 and ATG7 Are Essential for the Maintenance of Human CD34(+) Hematopoietic Stem-Progenitor Cells. *Stem Cells* **34**, 1651–1663 (2016).
12. Liu, F. *et al.* FIP200 is required for the cell-autonomous maintenance of fetal hematopoietic stem cells. *Blood* **116**, 4806–4814 (2010).
13. Vannini, N. *et al.* Specification of haematopoietic stem cell fate via modulation of mitochondrial activity. *Nat. Commun.* **7**, 13125 (2016).
14. Ho, T. T. *et al.* Autophagy maintains the metabolism and function of young and old stem cells. *Nature* **543**, 205–210 (2017).
15. Du, W. *et al.* The role of autophagy in targeted therapy for acute myeloid leukemia. *Autophagy* **17**, 2665–2679 (2021).
16. Liang, H. *et al.* Deciphering the Heterogeneity of Mitochondrial Functions During Hematopoietic Lineage Differentiation. *Stem cell Rev. reports* **18**, 2179–2194 (2022).
17. Sumitomo, Y. *et al.* Cytoprotective autophagy maintains leukemia-initiating cells in murine myeloid leukemia. *Blood* **128**, 1614–1624 (2016).
18. Nguyen, T. D. *et al.* Loss of the selective autophagy receptor p62 impairs murine myeloid leukemia progression and mitophagy. *Blood* **133**, 168–179 (2019).
19. Dubois, A. *et al.* LAMP2 expression dictates azacytidine response and prognosis in MDS/AML. *Leukemia* **33**, 1501–1513 (2019).
20. Auberger, P. & Puissant, A. Autophagy, a key mechanism of oncogenesis and resistance in leukemia. *Blood* **129**, 547–552 (2017).
21. Jao, L.-E., Wente, S. R. & Chen, W. Efficient multiplex biallelic zebrafish genome editing using a CRISPR nuclease system. *Proc. Natl. Acad. Sci. U. S. A.* **110**, 13904–13909 (2013).
22. Wu, R. S. *et al.* A Rapid Method for Directed Gene Knockout for Screening in G0 Zebrafish. *Dev. Cell* **46**, 112-125.e4 (2018).
23. Kuma, A. *et al.* The role of autophagy during the early neonatal starvation period. *Nature* **432**, 1032–

1036 (2004).

24. Piya, S. *et al.* Atg7 suppression enhances chemotherapeutic agent sensitivity and overcomes stroma-mediated chemoresistance in acute myeloid leukemia. *Blood* **128**, 126–1269 (2016).

25. Mortensen, M. *et al.* The autophagy protein Atg7 is essential for hematopoietic stem cell maintenance. *J. Exp. Med.* **208**, 455–467 (2011).

26. Ito, K. *et al.* Self-renewal of a purified Tie2+ hematopoietic stem cell population relies on mitochondrial clearance. *Science* **354**, 1156–1160 (2016).

27. Fan, S. *et al.* PINK1-Dependent Mitophagy Regulates the Migration and Homing of Multiple Myeloma Cells via the MOB1B-Mediated Hippo-YAP/TAZ Pathway. *Adv. Sci. (Weinheim, Baden-Wurttemberg, Ger.* **7**, 1900860 (2020).

28. Nunnari, J. & Suomalainen, A. Mitochondria: in sickness and in health. *Cell* **148**, 1145–1159 (2012).

29. Wang, D. *et al.* Antioxidants protect PINK1-dependent dopaminergic neurons in Drosophila. *Proc. Natl. Acad. Sci. U. S. A.* **103**, 13520–13525 (2006).

30. Gautier, C. A., Kitada, T. & Shen, J. Loss of PINK1 causes mitochondrial functional defects and increased sensitivity to oxidative stress. *Proc. Natl. Acad. Sci. U. S. A.* **105**, 11364–11369 (2008).

31. Heeman, B. *et al.* Depletion of PINK1 affects mitochondrial metabolism, calcium homeostasis and energy maintenance. *J. Cell Sci.* **124**, 1115–1125 (2011).

32. Grünewald, A. *et al.* Differential effects of PINK1 nonsense and missense mutations on mitochondrial function and morphology. *Exp. Neurol.* **219**, 266–273 (2009).

33. Stauch, K. L. *et al.* Loss of Pink1 modulates synaptic mitochondrial bioenergetics in the rat striatum prior to motor symptoms: concomitant complex I respiratory defects and increased complex II-mediated respiration. *Proteomics. Clin. Appl.* **10**, 1205–1217 (2016).

34. Grigoruţă, M., Dagda, R. K., Díaz-Sánchez, Á. G. & Martínez-Martínez, A. Psychological distress and lack of PINK1 promote bioenergetics alterations in peripheral blood mononuclear cells. *Sci. Rep.* **10**, 9820 (2020).

35. Poole, A. C. *et al.* The PINK1/Parkin pathway regulates mitochondrial morphology. *Proc. Natl. Acad.*

Sci. U. S. A. **105**, 1638–1643 (2008).

36. Pei, S. *et al.* AMPK/FIS1-Mediated Mitophagy Is Required for Self-Renewal of Human AML Stem Cells. *Cell Stem Cell* **23**, 86-100.e6 (2018).

37. Dykstra, K. M. *et al.* Inhibiting autophagy targets human leukemic stem cells and hypoxic AML blasts by disrupting mitochondrial homeostasis. *Blood Adv.* **5**, 2087–2100 (2021).

38. Yi, Z.-N., Chen, X.-K. & Ma, A. C.-H. Modeling leukemia with zebrafish (Danio rerio): Towards precision medicine. *Exp. Cell Res.* **421**, 113401 (2022).

39. Wang, D. *et al.* Transgenic IDH2(R172K) and IDH2(R140Q) zebrafish models recapitulated features of human acute myeloid leukemia. *Oncogene* (2023) doi:10.1038/s41388-023-02611-y.

40. Kimmel, C. B., Ballard, W. W., Kimmel, S. R., Ullmann, B. & Schilling, T. F. Stages of embryonic development of the zebrafish. *Dev. Dyn. an Off. Publ. Am. Assoc. Anat.* **203**, 253–310 (1995).

41. Chen, X.-K., Kwan, J. S.-K., Chang, R. C.-C. & Ma, A. C.-H. 1-phenyl 2-thiourea (PTU) activates autophagy in zebrafish embryos. *Autophagy* **17**, 1222–1231 (2021).

42. Ma, A. C. H., Ward, A. C., Liang, R. & Leung, A. Y. H. The role of jak2a in zebrafish hematopoiesis. *Blood* **110**, 1824–1830 (2007).

43. He, C. & Klionsky, D. J. Analyzing autophagy in zebrafish. *Autophagy* **6**, 642–644 (2010).

44. Khuansuwan, S., Barnhill, L. M., Cheng, S. & Bronstein, J. M. A novel transgenic zebrafish line allows for in vivo quantification of autophagic activity in neurons. *Autophagy* **15**, 1322–1332 (2019).

45. Purushothaman, K. *et al.* Proteomics Analysis of Early Developmental Stages of Zebrafish Embryos. *Int. J. Mol. Sci.* **20**, (2019).

46. Fan, P.-C. *et al.* Liquid Chromatography Tandem Mass/Mass Spectrometry for the Quantification of Fudosteine in Human Serum without Precolumn Derivatization. *Iran. J. Pharm. Res. IJPR* **13**, 441–447 (2014).

47. Gibert, Y., McGee, S. L. & Ward, A. C. Metabolic profile analysis of zebrafish embryos. *J. Vis. Exp.* e4300 (2013) doi:10.3791/4300.

48. Bond, S. T., McEwen, K. A., Yogananthajah, P. & Gibert, Y. Live Metabolic Profile Analysis of

Zebrafish Embryos Using a Seahorse XF 24 Extracellular Flux Analyzer. *Methods Mol. Biol.* **1797**, 393–401 (2018).

Acknowledgements

The Fish Model Translational Research Laboratory (HTI, POLYU) maintains the aquatic facility and zebrafish strains. The University Research Facility in Life Sciences and the University Research Facility (ULS, POLYU) in Chemical and Environment Analysis (UCEA, POLYU) provides the Leica TCS SPE Confocal Microscope, BD FACSAria III Cell Sorter, LC/ESI - QTrap Mass Spectrometer, Zeiss Lightsheet 7 Selective Plane Illumination Microscope, and services.

Funding Support

This study is supported by FHB Health and Medical Research Fund (03143765, 06173226) and RGC Theme-based Research Scheme (T12-702/20-N) to ACM.

Authorship contributions

A.M. conceptualized and supervised the study, and rote the manuscript. Z.Y. and X.C. designed and performed the experiments, prepared the figures, and wrote the manuscript. All authors reviewed and revised the manuscript.

Conflict of Interest Disclosures

The authors declare no competing interests.

Figure Legends

Figure 1. Targeting *pink1* affects autophagic levels of whole embryos, muscle, and blood cells in zebrafish.

a, the protein structure of human and zebrafish PINK1. Identity and similarity shared by the human PINK1, and

the zebrafish *pink1* protein sequence are shown in percentage. I, percent identity; S, percent similarity. **b**, the schematic graph of sgRNA designed targeting zebrafish *pink1* gene. The binding site of sgRNA locates in the exon3 of the zebrafish *pink1* gene, within which the enzyme AciI was used for the RELP assay. **c** RFLP result confirmed nearly 100% efficiency of knockouts. **d** and **e**, the result of western blot against the PINK1 antibody showed nearly 100% reduced expression in 48 hpf *pink1* mutants. Western blot showed an increased LC3B/GAPDH ratio in *pink1* mutants, indicating elevated autophagy in whole lysates. **f** and **g**, Lightsheet microscopy of muscle region from 4 dpf zebrafish, with Lysotracker staining the autolysosome compartments, in CTRL and *pink1* mutants. RNP was delivered into Tg(Lc3:EGFP) zebrafish line. The autophagic levels were indicated by counted puncta with merged signals per muscle area. **h**, the schematic graph of monitoring autophagy in blood cells from zebrafish embryos. RNP was delivered into the Tg(*coro1a*:DsRed) zebrafish embryos at the 1-cell stage. Embryos were raised to 2 dpf and screened for *coro1a*: DsRed positive signals. Then the embryos were dissociated to sort the hematopoietic cells, stained with CYTO-ID, and imaged via confocal. **i**, Confocal microscopy of autophagic structure in hematopoietic cells of CTRL and mutant embryos. **j**, the quantitative result of LC3:GFP positive puncta per myeloid cell. CTRL, control. Mut, mutant. CQ, chloroquine. RFLP, restriction fragment length polymorphism. ns, not significant. n=20~40. Scale bar: 20 um. *p≤0.05, **p≤0.01, ***p≤0.001, two-tailed Student's t-test.

Figure 2. *pink1* mutated embryos showed expanded definitive hematopoiesis that can be rescued by autophagy inhibitors. **a-d**, Whole mount in situ hybridization (WISH) testing against *hbae1, l-plastin, c-myb*, and *mpx* probes in 48 hpf zebrafish embryos, with or without 3-Methyladenine (3-MA, 10mM), autophagy inhibitor. The enlarged picture indicates areas selected for quantification. **e**, the quantitative analysis of WISH results showed increased expression of *hbae1, l-plastin,* and *c-myb* in 48 hpf *pink1* mutant zebrafish embryos. Lateral view, head to left, mutants and siblings. Line denotes the mean value. p<0.01, n=20~40. CTRL, control. Mut, mutant. *p⩽0.05, **p⩽0.01, compared to control, #p⩽0.05, ## p⩽0.01, compared to mutant, $$ p⩽0.01, compared to 3-MA group, two-tailed Student's t-test.

Figure 3. *pink1* mutants show increased oxidative phosphorylation. a, the schematic graph of Sea horse mitochondrial stress test with whole zebrafish embryos. In a 24-well plate, there are 4 negative controls with no embryos, 5 control embryos, and 5 *pink1* mutant embryos, on the bottom of the plate locked with a net. Oligomycin, FCCP, and Rotenone/AA were added consecutively. **b**, the oxygen consumption rate measured over time in the mitochondrial stress test of live embryos. The black line represents control, the red line represents the *pink1* mutants. Zebrafish at 48 hpf. Mean values +- SEM. N=5. **c**, basal respiration. **d**, maximal respiration. **e**, ATP production. **f**, coupling efficiency (%). **g**, spare respiratory capacity (%). **h**, the schematic graph showed the method to monitor mitochondrion in zebrafish. Mitored mRNA was delivered into Tg(*mfap4*:BFP) zebrafish embryos. **i**, Confocal images of mitochondrial structures among muscle area of CTRL and *pink1* mutant Tg(*mfap4*:BFP) zebrafish embryos. Dpf, days past fertilization. FCCP, carbonyl cyanide 4-(trifluoromethoxy-phenylhydrazone). AA, antimycin A. CTRL, control. Mut, mutant. n=20, *p⩽0.05,**p⩽0.01, two-tailed Student's t-test.

Figure 4. *pink1* mutants show proteomic changes that can explain the observed phenotypes. **a**, the schematic graph showed the method of mass spectrometry (MS)-based proteomics in zebrafish. RNP was delivered into wild-type embryos by microinjection, then proteins extracted from 2 dpf embryos were purified, and digested by trypsin to run on the liquid chromatography (LC)-target free-time of flight (TOF) mass spectrum. Data analyses were run against the zebrafish protein sequence database. **b**, the volcano plot of p-values (-log10) and z-scores (log2) in quantified proteins between CTRL and *pink1* mutants. The dots located on top of the dashed line represent significantly differentiated expressed proteins ($p<0.05$, z-score>1.2). **c-e**, the heat map of significantly altered proteins from, mitochondrial, cell cycle, and proliferation, and metabolism pathways among 3 biological replicates between mutant and CTRL groups. CTRL, control. Mut, mutant. n=30, two-tailed Student's t-test was used between groups.

Figure 5. Targeting *PINK1* induces cell proliferation and autophagy in AML cells. a, the schematic graph of creating *PINK1* mutated leukemic cell line via CRISPR/cas9 technique. sgRNA targets early exon of the human *PINK1* gene. sgRNA mixed with cas9 protein forms the RNP complexes. RNP was delivered into OCI-AML cells via electroporation (Neon transfection). **b**, the result of restriction fragment length polymorphism (RFLP) assay. CRTL showed fully cleaved DNA bands while the *PINK1* mutant showed uncleaved bands (efficiency over 90%). **c** and **d**, PINK1 deficiency verified by western blot against PINK1 antibody. GAPDH antibody serves as the internal control. **e**, the results of Flow cytometry. Cells are treated with or without chloroquine (CQ) and stained with Cyto-ID, a dye specifically marks autophagic vacuoles. The percentage indicates increased autophagic flux in *PINK1* mutated cells compared to the control, treated with or without CQ. **f**, Confocal imaging showed increased autophagic flux in *PINK1* mutated leukemic cells, with or without treatment of CQ. **g** and **h**, the statistical analysis of autophagic flux. **i**, plot showed the rates of proliferation (fold change by 24 hours). Data are shown as mean of three independent experiments. Mean values SEM. CTRL, control. Mut, mutant. CQ, chloroquine. *$p \leqslant 0.05$, **$p \leqslant 0.01$, two-tailed Student's t-test.

Figure 1.

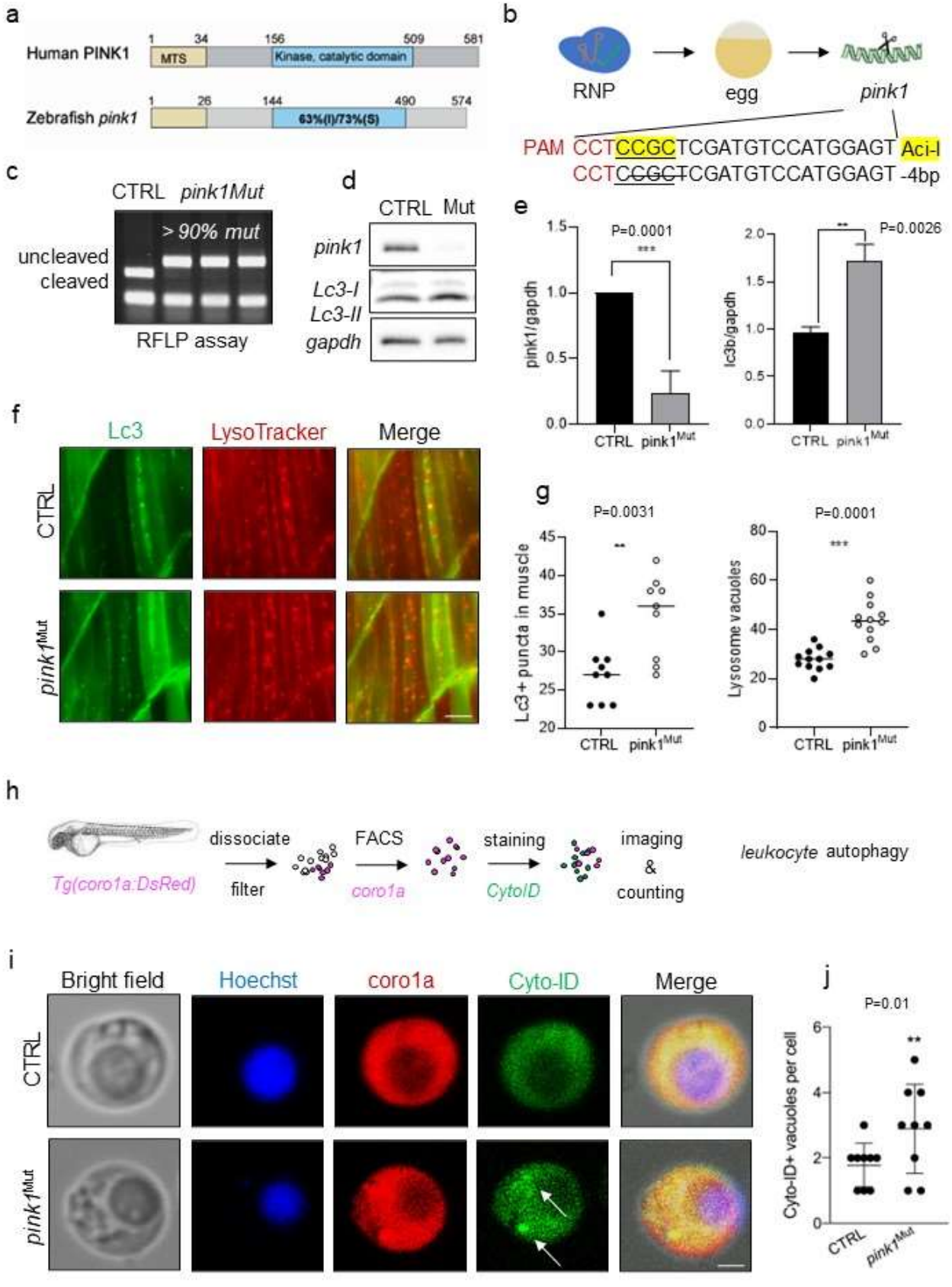
a
Human PINK1
MTS
Kinase, catalytic domain
Zebrafish pink1
63%(I)/73%(S)
b
RNP
egg
pink1
PAM CCTCCGCTCGATGTCCATGGAGT Aci-I
CCTCCGCTCGATGTCCATGGAGT -4bp
c
CTRL pink1Mut
> 90% mut
uncleaved
cleaved
RFLP assay
d
CTRL Mut
pink1
Lc3-I
Lc3-II
gapdh
e
P=0.0001
P=0.0026
pink1/gapdh
lc3b/gapdh
CTRL pink1Mut
f
Lc3
LysoTracker
Merge
CTRL
pink1Mut
g
P=0.0031
P=0.0001
Lc3+ puncta in muscle
Lysosome vacuoles
h
Tg(coro1a:DsRed)
dissociate
filter
FACS
coro1a
staining
CytoID
imaging
&
counting
leukocyte autophagy
i
Bright field
Hoechst
coro1a
Cyto-ID
Merge
CTRL
pink1Mut
j
P=0.01
Cyto-ID+ vacuoles per cell

Figure 2.

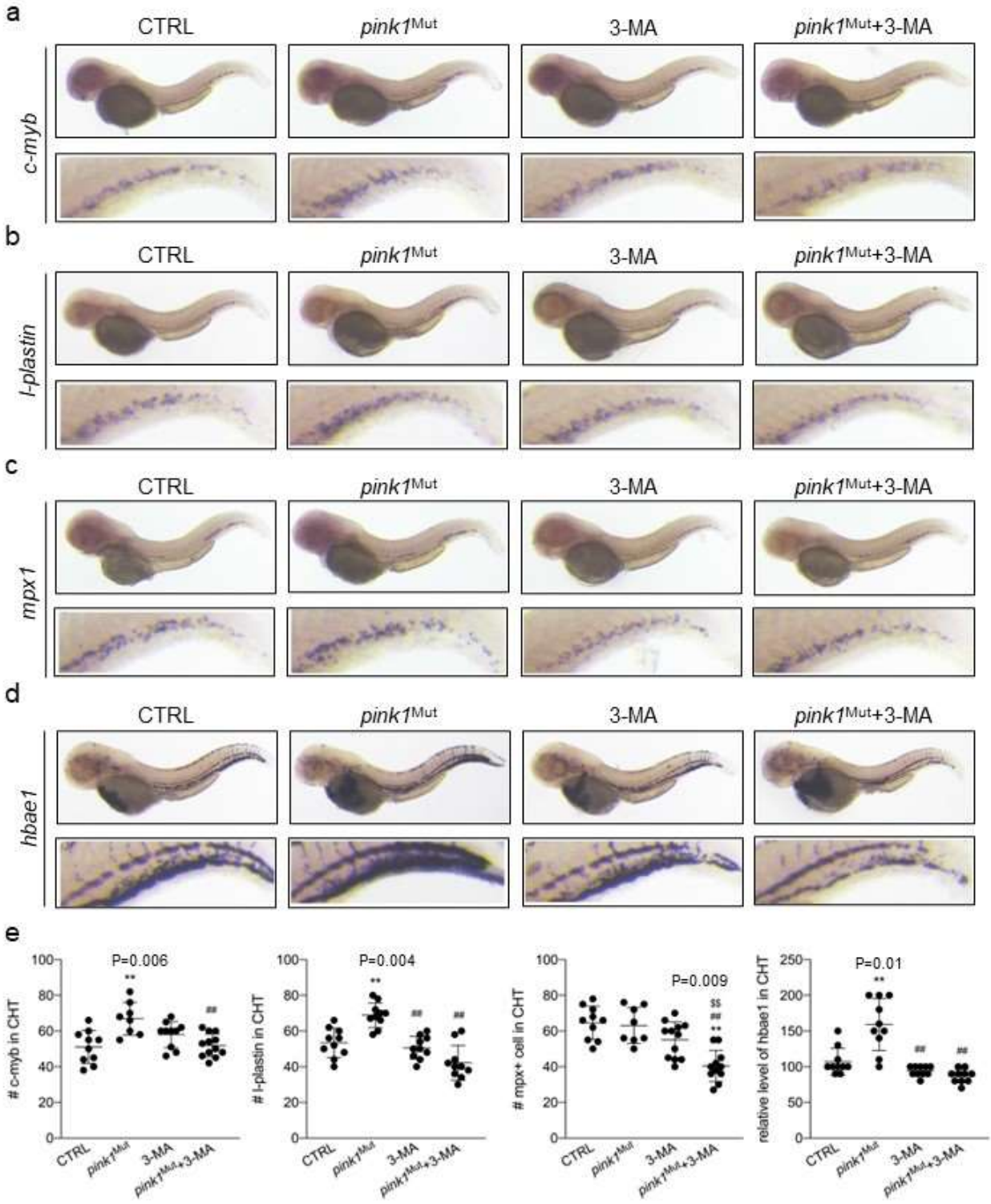
a
CTRL
pink1Mut
3-MA
pink1Mut+3-MA
c-myb
b
CTRL
pink1Mut
3-MA
pink1Mut+3-MA
l-plastin
c
CTRL
pink1Mut
3-MA
pink1Mut+3-MA
mpx1
d
CTRL
pink1Mut
3-MA
pink1Mut+3-MA
hbae1
e
P=0.006
# c-myb in CHT
P=0.004
# l-plastin in CHT
P=0.009
# mpx+ cell in CHT
P=0.01
relative level of hbae1 in CHT
CTRL
pink1Mut
3-MA
pink1Mut+3-MA

Figure 3.

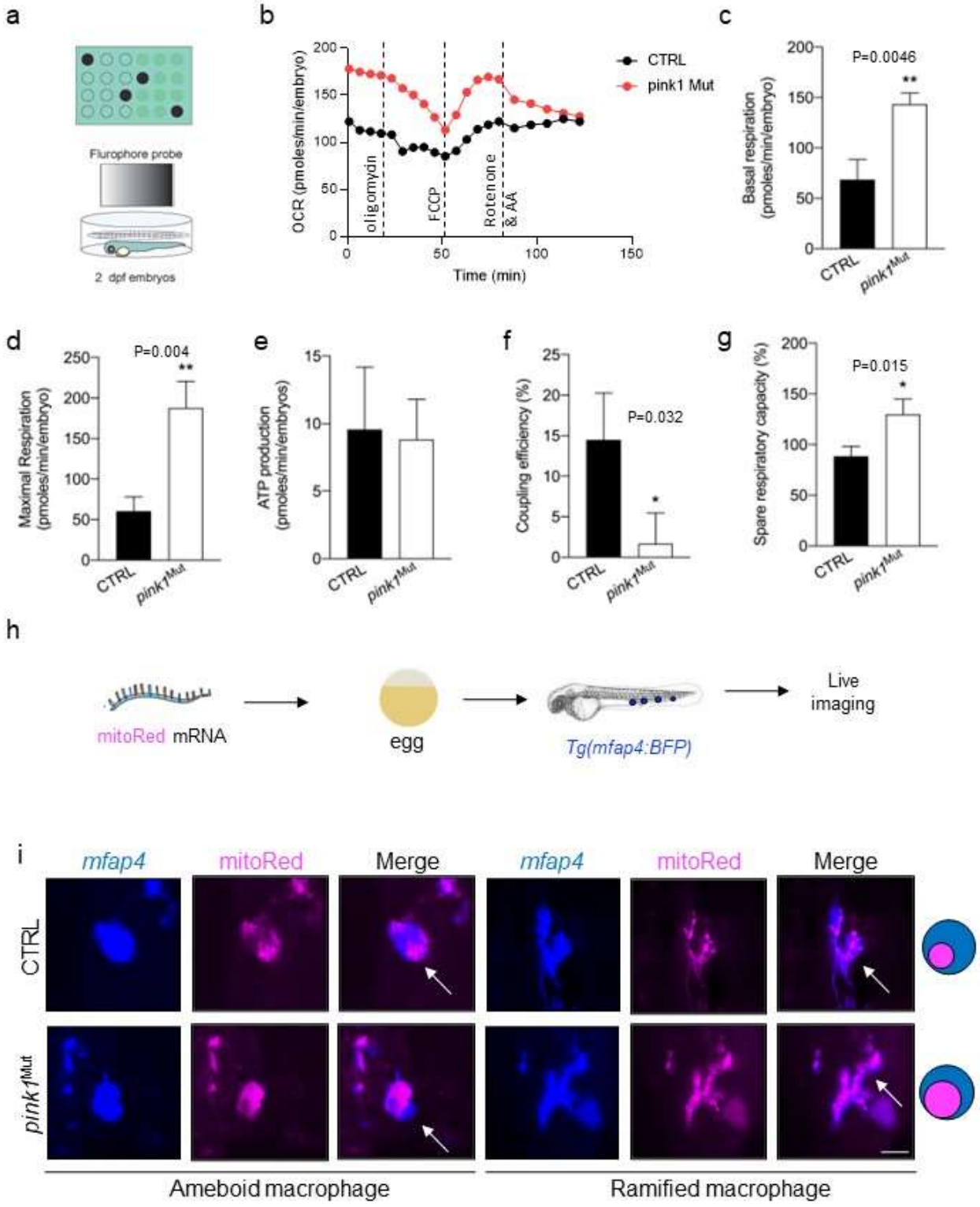
a
Flurophore probe
2 dpf embryos
b
OCR (pmoles/min/embryo)
oligomydin
FCCP
Rotenone & AA
Time (min)
CTRL
pink1 Mut
c
Basal respiration (pmoles/min/embryo)
P=0.0046
**
CTRL
pink1Mut
d
Maximal Respiration (pmoles/min/embryo)
P=0.004
**
e
ATP production (pmoles/min/embryos)
f
Coupling efficiency (%)
P=0.032
*
g
Spare respiratory capacity (%)
P=0.015
*
h
mitoRed mRNA
egg
Tg(mfap4:BFP)
Live imaging
i
mfap4
mitoRed
Merge
CTRL
pink1Mut
Ameboid macrophage
Ramified macrophage

Figure 4.

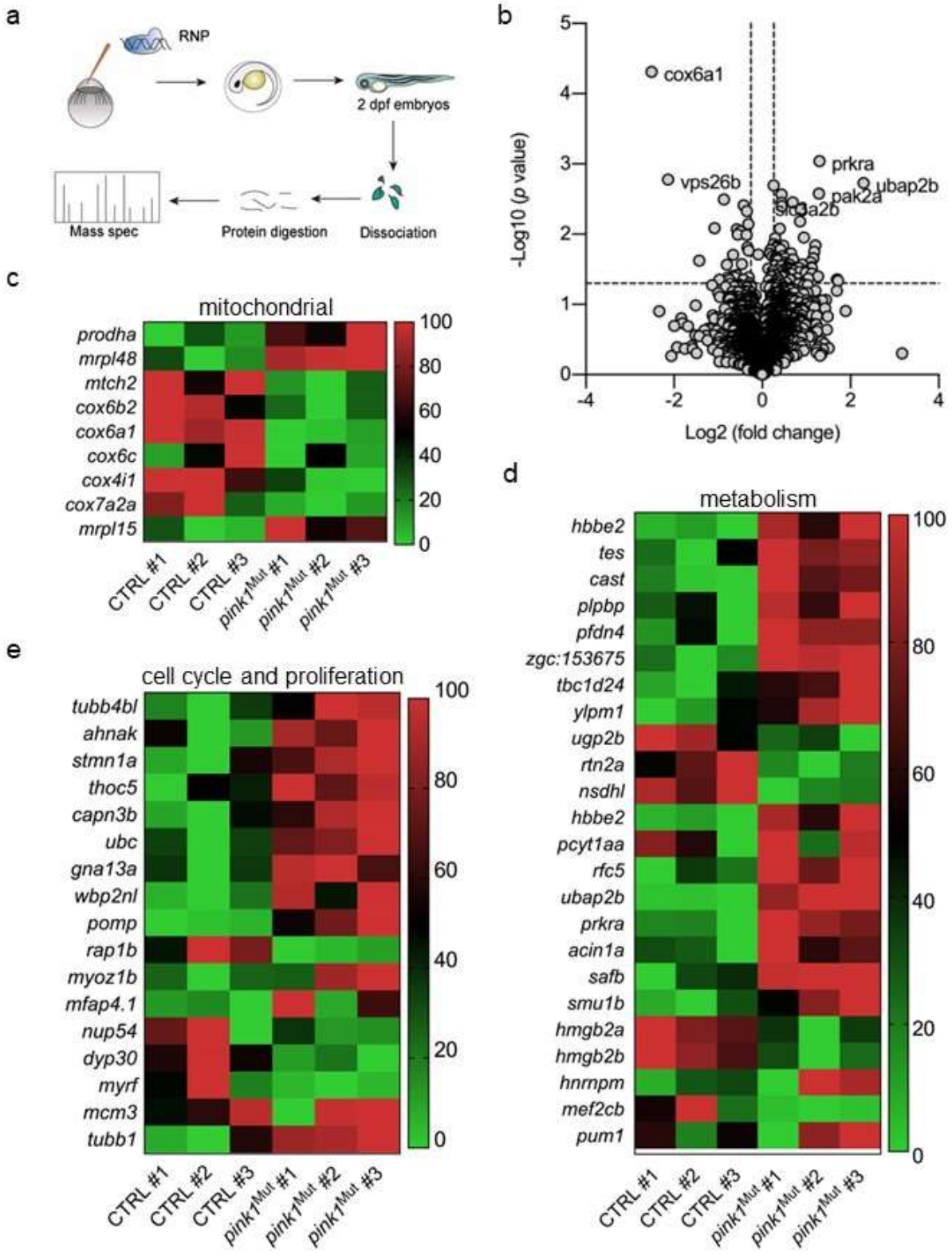
a
RNP
2 dpf embryos
Dissociation
Protein digestion
Mass spec
b
cox6a1
prkra
vps26b
ubap2b
pak2a
-Log10 (p value)
Log2 (fold change)
c
mitochondrial
prodha
mrpl48
mtch2
cox6b2
cox6a1
cox6c
cox4i1
cox7a2a
mrpl15
CTRL #1
CTRL #2
CTRL #3
pink1Mut #1
pink1Mut #2
pink1Mut #3
d
metabolism
hbbe2
tes
cast
plpbp
pfdn4
zgc:153675
tbc1d24
ylpm1
ugp2b
rtn2a
nsdhl
hbbe2
pcyt1aa
rfc5
ubap2b
prkra
acin1a
safb
smu1b
hmgb2a
hmgb2b
hnrnpm
mef2cb
pum1
e
cell cycle and proliferation
tubb4bl
ahnak
stmn1a
thoc5
capn3b
ubc
gna13a
wbp2nl
pomp
rap1b
myoz1b
mfap4.1
nup54
dyp30
myrf
mcm3
tubb1

Figure 5.

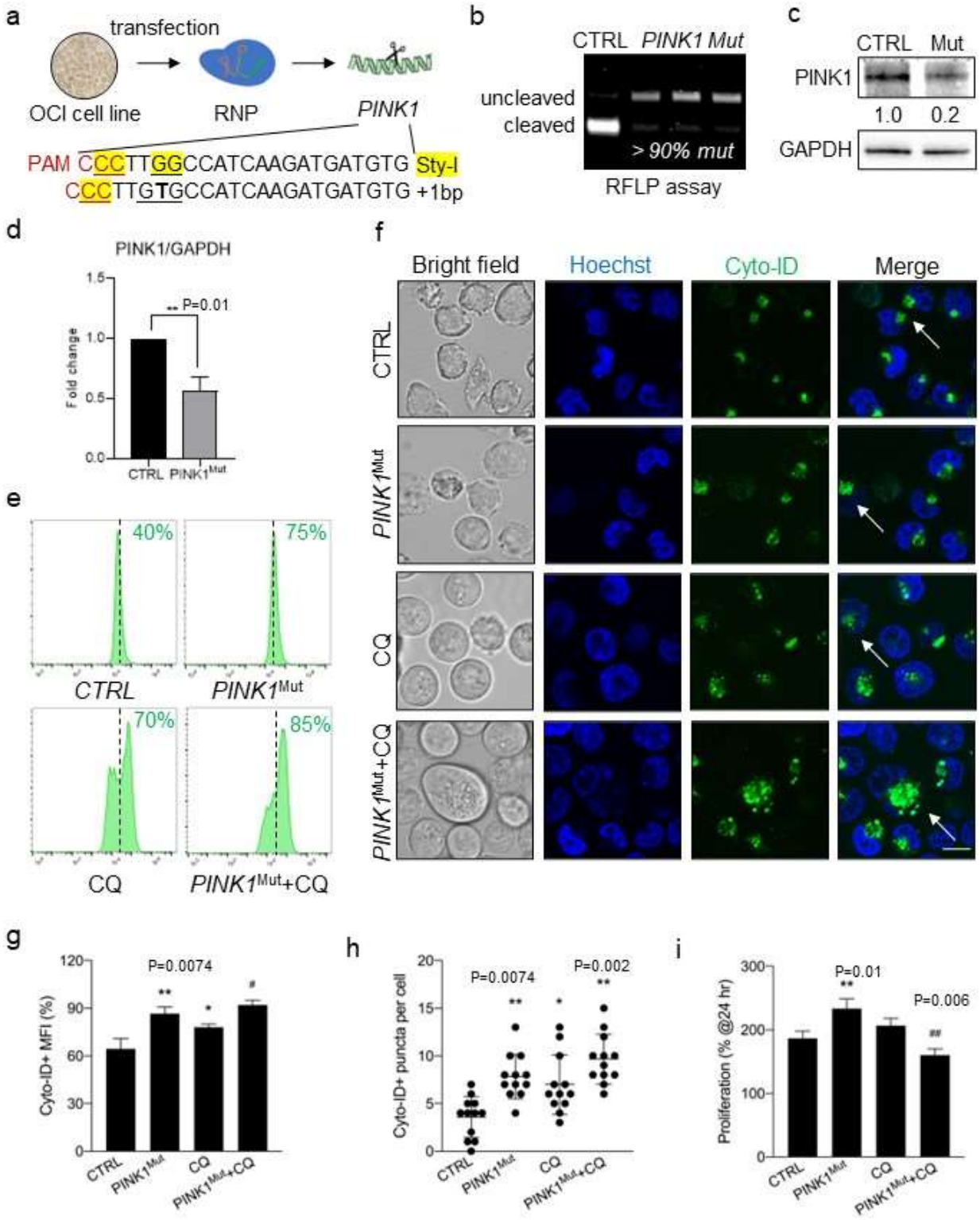
a
transfection
OCI cell line
RNP
PINK1
PAM CCCTTGGCCATCAAGATGATGTG Sty-I
CCCTTGTGCCATCAAGATGATGTG +1bp
b
CTRL PINK1 Mut
uncleaved
cleaved
> 90% mut
RFLP assay
c
CTRL Mut
PINK1
1.0 0.2
GAPDH
d
PINK1/GAPDH
Fold change
** P=0.01
CTRL PINK1Mut
e
40%
75%
CTRL
PINK1Mut
70%
85%
CQ
PINK1Mut+CQ
f
Bright field
Hoechst
Cyto-ID
Merge
CTRL
PINK1Mut
CQ
PINK1Mut+CQ
g
Cyto-ID+ MFI (%)
P=0.0074
CTRL PINK1Mut CQ PINK1Mut+CQ
h
Cyto-ID+ puncta per cell
P=0.0074
P=0.002
CTRL PINK1Mut CQ PINK1Mut+CQ
i
Proliferation (% @24 hr)
P=0.01
P=0.006
CTRL PINK1Mut CQ PINK1Mut+CQ

Supplementary Files

This is a list of supplementary files associated with this preprint. Click to download.

- YietalSupplementalMaterial.pdf